Available online at www.sciencedirect.com
SCIENCE DIRECT®
Optics Communications 253 (2005) 308–314
OPTICS COMMUNICATIONS
www.elsevier.com/locate/optcom

Efficient mode coupling technique between photonic crystal heterostructure waveguide and silica waveguides

Yuan-Fong Chau [a,*], Tzong-Jer Yang [b], Ben-Yuan Gu [c], Win-Der Lee [a]

[a] Department of Electrical Engineering, Lee-Ming Institute of Technology, Taipei, Taiwan, Republic of China
[b] Department of Electrophysics, National Chiao Tung University, Hsinchu, Taiwan, Republic of China
[c] Institute of Physics, Chinese Academy of Sciences, P.O. Box 603, Beijing 100080, China

Received 26 August 2004; received in revised form 6 April 2005; accepted 27 April 2005

Abstract

We report an efficient mode coupling technique between silica waveguides (SWGs) and a planar photonic crystal heterostructure waveguide (PPCHWG) composed of two semi-infinite two-dimensional photonic crystals (PCs) with different filling fractions. By calculating the transmittance at output end of SWG, we find that the designed structures possess the merits of high coupling efficiency and relaxing fabricating tolerance. The maximal transmittance exceeds 90% at a wavelength near 1.65 μm. The high transmission efficiency of PPCHWGs can be achieved without introducing any defect structures for optimal mode matching. Besides, the width of PPCHWGs can be flexibly adjusted via changing the separation of two component PCs in PC heterostructures.

PACS: 78.20.Ci; 78.20.Bh

Keywords: Photonic crystal; Silica waveguide; Heterostructure waveguide; Transmission efficiency

Photonic crystals (PCs) can be served to various micro-optical components and micro-circuits [1–5], for example, planar photonic crystal waveguides (PPCWGs) [6–9] have been widely applied to guiding the propagation of light waves via line structural defects. To construct efficient integrated optical circuits (IOCs), the high coupling efficiency is desired as losses always occur at any interfaces between different components in waveguides. For instance, PPCWGs have to connect to the conventional silica waveguides (SWGs) at their entrance and exit ends in practical optical communication elements. Therefore, acquiring optimal power

* Corresponding author. Tel.: +886 429097811; fax: +886 422967582.
E-mail addresses: yfchau@mail.apol.com.tw (Y.-F. Chau), yangtj@cc.nctu.edu.tw (T.-J. Yang).

0030-4018/$ - see front matter © 2005 Elsevier B.V. All rights reserved.
doi:10.1016/j.optcom.2005.04.080

conversion among the external wires and the PPCWGs still is a challenge task. There are various schemes proposed for arriving at this goal, for instance, enlarging the band gap size, promoting the transmission efficiency, and reducing back-reflections arising from mode mismatching at interfaces between PPCWGs and SWGs. The improved coupling structure in the PPCWGs has been presented and experimentally verified [6,9], by gradually varying the rod size at the ends of the PPCWGs. Furthermore, a coupling technique, which is based on employing four in-axis (in the W1-direction, where W1 means that one row of dielectric rods along the propagation direction is removed) circular defect rods [7] and twelve off-axis (away from the W1-direction) elliptical Si defect rods [8] in combination with adjusting the radii and positions of defects within the conventional PPCWG tapers, has been reported. Although a high peak transmission up to 80% was obtained over a certain finite frequency range, it is still difficult to construct optimal tapered structures and control the rod sizes at the desired accuracy in practical fabrications. In addition, the extra procedures of altering the rod sizes and positions of dielectric rods should lead to complexity and difficulty in the fabrications. Especially, higher expanses may be paid to realize IOCs. How to simplify the fabrication processes and lower the manufacturing cost becomes one of the important issues.

Inspired by these active issues, in this paper, we propose a planar photonic crystal heterostructure waveguide (PPCHWG) consisting of two semi-infinite PCs with different structural parameters, which is connected to two external SWGs. PPCHWGs possess ability of flexible creation of the defect states by changing structural parameters of two component PCs in heterostructure. Unlike the conventional two-dimensional (2D) PCWGs formed by removing some rods or air holes in lines, the width of the WGs cannot be continuously or linearly altered owing to the discrete variation of the number of the defect lines. However, the PPCHWGs are formed by introducing relatively longitudinal gliding of the cylinders in the lattices on the two sides of the interface of heterostructure (referred to the longitudinal gliding of lattices) or displacing the cylinders in the lattices on either sides of the interfaces (referred to the transverse displacement of lattices). Consequently, the width of the PPCHWGs can be artificially adjusted for obtaining maximal coupling efficiency.

In photonic crystal heterostructures, the perfect periodical modulation of dielectric function is broken at the interface, thus, strong scattering of electromagnetic (EM) waves occurs. The interference between the scattering EW waves leads to the creation of the localized interfacial states, which can be served as guiding the propagation of light waves along the interface, i.e., light wave guides. In the 3D photonic band gap structure [11], the face-centered-cubic photonic band gap crystals with overlapping stop band can be stacked in tandem to obtain an ultrawide band PC. Recently, Zhang et al. [12] indicated theoretically that omnidirectional total reflection frequency range can be significantly enlarged by combining two or more one-dimensional (1D) PCs, whose omnidirectional PBGs may be bridged to connect each other. In addition, inserting multiple photonic quantum-wells into 1D PCs can generate the defect modes in the omnidirectional PBGs [10].

For the simplicity of the analysis, we only focus on the 2D PC heterostructures. The proposed coupling structure between SWG and PPCHWG is shown schematically in Fig. 1. The PPCHWG is composed of two semi-infinite PCs made by GaAs cylinders of the refractive index $n = 3.4$ in a square lattice (with a lattice constant of a) embedded in air. Two semi-infinite PCs have the complete identical structural parameters only except for the difference of the filling fractions, denoted by f_1 and f_2. The SWG consists of Silica with a dielectric index of 1.45, its width is 2.5 μm, surround by air. As is well known [13,14], a good tapered structure plays a critical role in achieving better mode matching between the fundamental modes of the wide dielectric SWG and those of the much narrower PPCWG. From the field patterns in the tapered region of the PPC, one finds that the adiabatical reduction of the cross section of the dielectric waveguide occurs in a relatively short distance, while still retaining almost perfect throughout. To acquire the optimal mode coupling between the PPCHWG and SWG, the suggested coupling

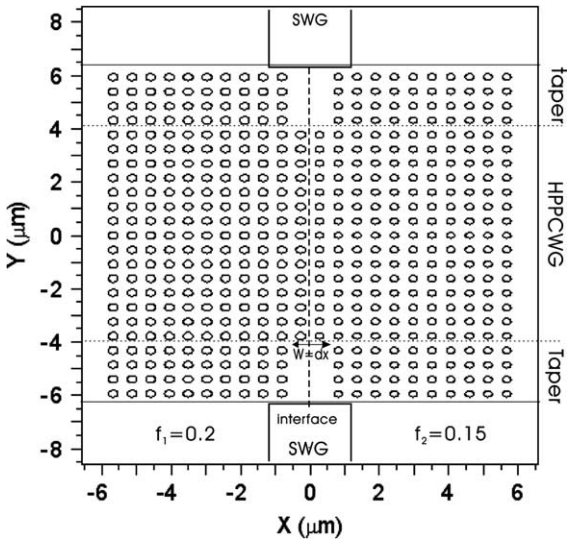

Fig. 1. Schematic view of a planar photonic crystal heterostructure waveguide (PPCHWG), connected to two external SWGs. The PPCHWG is composed of two semi-infinite PCs made by GaAs cylinders of the refractive index $n = 3.4$ in a square lattice (with a lattice constant of a) embedded in air. Two semi-infinite PCs have the complete identical structural parameters only except for the difference of the filling fractions, denoted by f_1 and f_2. The SWG consists of Silica with a dielectric index of 1.45, its width is 2.5 μm, surround by air. The suggested coupling structures at the entrance and exit terminals of the PPCHWG is a stepwise taper formed by removing four rods of the original PPCHWG at the entrance and exit ends of it in the y-direction. The y-axis is chosen parallel to the interface and the x-axis is normal to the interface.

structures at the entrance and exit terminals of the PPCHWG are displayed in Fig. 1; a stepwise taper is formed by removing four rods of the original PPCHWG at the entrance and exit ends of it in the y-direction.

By using the plane-wave expansion [15] method in combination with supercell technique, we calculate the photonic band gaps (PBGs) and find that the PBG is laid in the range of $a/\lambda = [0.262, 0.377]$ or $\lambda \in [1.432, 2.06]$ μm along the Γ–X-direction for the TM (in-plane magnetic field) polarization. The parameters are chosen as: $f_1 = 0.2$, (i.e., the radius of the dielectric cylinders is $r_1 = 136$ nm), and $f_2 = 0.15$, (i.e., $r_2 = 118$ nm); $a = 540$ nm. The value $(f1, f2) = (0.2, 0.15)$ is chosen in such a way that the largest gap is produced; in this situation, the defect mode is easily survived and much stable within the large gap. As reported in [10] and [16,17], any guided modes cannot be generated when not introducing relatively longitudinally gliding dx or transverse displacement dy of lattices together with cylinders on either sides of the interface of PPCH to the host medium.

The generation of localized interfacial modes is indispensable condition for serving as waveguides. Thus, we now introduce several relatively transverse displacements of $dx = 0.5a$, $dx = 0.7a$, $dx = 1.0a$, $dx = 1.3a$, $dx = 1.44a$, and $dx = 3.0a$. The calculated photonic band structures are displayed in Fig. 2(a)–(f) for the TM polarization. The distributions of the relevant EM fields are also displayed in the inset of Fig. 2(a)–(f) for reference. It is evident that the guided modes exhibit strong localization behavior demonstrated in Fig. 2(c), (d), and (e), which correspond to $dx = 1.0a$, $dx = 1.3a$, and $dx = 1.44a$, respectively.

To gain the mode coupling of high conversion efficiency between the PPCHWG and SWGs, the suggested coupling structures at the entrance and exit terminals of the PPCHWG are produced by removing four rods on either sides of the interface of the PPCH along the y-axis in one line and from two ends. We calculate the transmission of system in terms of 2D finite-difference time-domain (FDTD) algorithm [18]. We assume that a TM polarized Gaussian wave packet with appropriate waveguide mode pattern is launched normally into the entrance terminal of the PPCHWG from the input end of SWG. Perfectly matched layer (PML) conditions have been adopted to prevent unwanted reflections from occurring [19]. The transmission spectrum is obtained from the Fourier transformed time series and it is normalized with respect to the launched source.

To find the optimal mode coupling conditions, we now change the relatively transverse displacement dx, for different operating wavelengths. The calculated power transmission as a function of the width of PPCHWG, i.e., dx, is depicted in Fig. 3. Three different operation wavelengths are assumed: the dashed-(solid-, dotted-) curve corresponds to the fundamental mode of the SWG, which is excited by a sinusoidal monochromatic continuous wave with a normalized power in the y-direction (see Fig. 1) [20]. The transmission is

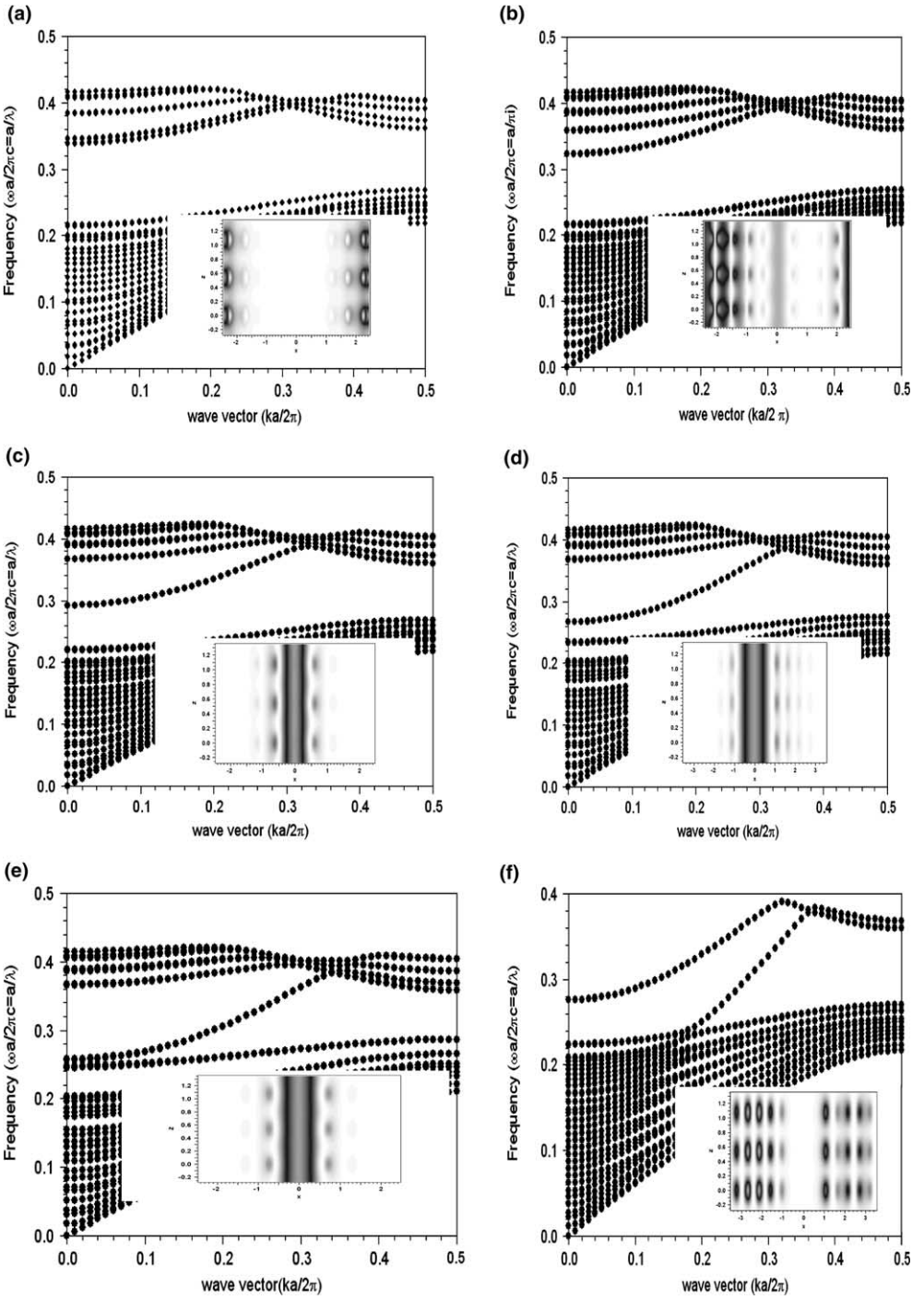

Fig. 2. Corresponding projected band structure and defect mode for the considered system, in which the transverse displacement between two semi-infinite PCs is taken as: (a) dx = 0.5a, (b) dx = 0.7a, (c) dx = 1.0a, (d) dx = 1.3a, (e) dx = 1.44a, and (f) dx = 3.0a, respectively. The parameters of the system are a = 540 nm, f_1 = 0.2, f_2 = 0.15, and n=3.4, and EM waves are assumed to be TM polarization.

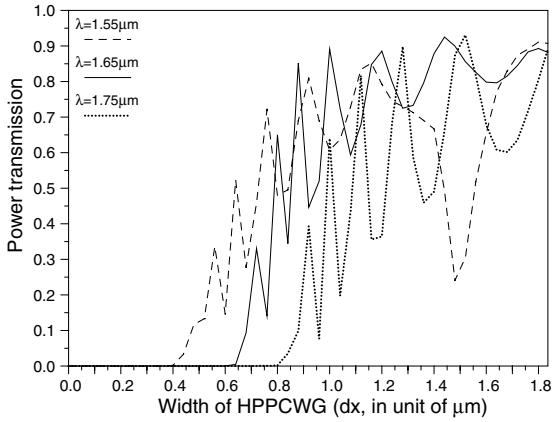

Fig. 3. Calculated power transmission as a function of the width of PPCHWG , which has been optimized at the central wavelength of $\lambda = 1.55$ μm (the dashed curve), $\lambda = 1.65$ μm (solid curve), and $\lambda = 1.75$ μm (dotted curve), respectively. The transmission is measured at output end of SWG of a monochromatic continuous-wave with a normalized power.

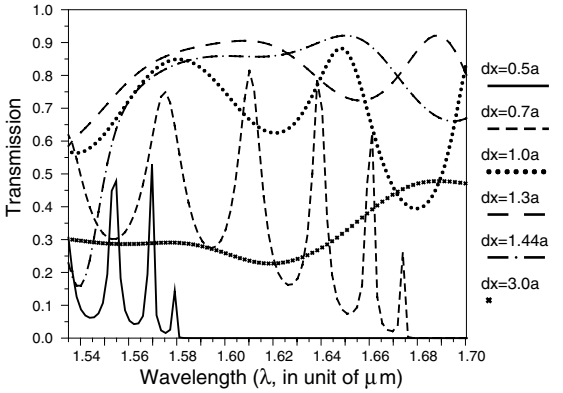

Fig. 4. Transmission spectrum of a PPCHWG of five different widths ($w = dx$), $dx = 0.5a$ (solid curve), $dx = 0.7a$ (dashed curve), $dx = 1.0a$ (dotted curve), $dx = 1.3a$ (long dashed curve), $dx = 1.44a$ (dash-dotted curve), and $dx = 3a$ (cross curve) at the optimum central wavelength of $\lambda = 1.65$ μm, coupling to an input and output SWG. The fundamental mode of the SWG is excited by a pulsed wave and the transmission spectrum is calculated with the evaluation of the overlap integral between the launched and measured fields at the output end of SWG.

measured at the output end of SWG (i.e., at $(x, y) = (0.9)$, as shown in Fig. 1). It is clearly seen from Fig. 3 that there exists a threshold of the PPCHWG width ($w = dx$), below it the transmission becomes forbidden because there is not any guide mode to be formed within the PBG of PPCH. In the simulations, we observe the fact that the width (dx) of the PPCHWG plays a critical role in changing the coupling efficiency of the system.

When increasing the dx, the transmission is rapidly increased in a heavy oscillatory manner. The occurrence of these oscillatory peaks can be attributed to the formation of the resonance cavity formed by the junctions between the SWG and PPCHWGs at the interface of heterostructure. With the increase of the operation wavelength, the onset threshold in the transmission spectrum is shifted toward the large width region. The better performance with an average transmission level of 73.83% is achieved over the width range of $w = dx = \in[1.143,1.83]$ μm and the maximum transmission is up to 93% at the operation wavelength $\lambda = 1.65$ μm.

To further explore the merits of the presented coupling system, we demonstrate the variations of the transmission spectrum of a PPCHWG as a function of the wavelength for six different widths, which corresponds to those values of dx appearing in Fig. 2, i.e., $w = dx = 0.5a$ for the solid curve, $dx = 0.7a$ for the dashed curve, $dx = 1.0a$ for the dotted curve, $dx = 1.3a$ for the long-dashed curve, $dx = 1.44a$ for the dash–dotted curve, and $dx = 3a$ for the cross curve, respectively. Here, the optimal center wavelength of $\lambda = 1.65$ μm obtained in Fig. 3 is employed. The fundamental mode of the SWG is excited by a pulse wave, propagating along the y-axis. The transmission spectrum is calculated by the evaluation of the overlap integral between the launched and measured fields at the exit end of the SWG. It is evident from Fig. 4 that all the curves exhibit oscillations with λ, containing series of sharp peaks. There exists a cut-off wavelength for each given width of the PPCHWG. The lower the cut-off wavelength, the narrower the PPCHWG width is. The oscillations are due to reflection coming from the modal mismatch between the wide PPC taper, where four rods have been removed, and the narrow PPCHWG. When the dx is increased, the reflection coefficient is reduced accordingly, therefore, the fringe contrast should be decreased. As increasing the width (dx) of the PPCHWG, the amplitude of the oscillations

becomes small and the average level of the transmission is significantly raised. The maximal transmittance can reach as high as 93% when the width $w = dx = 1.44a$ of the PPCHWG. We also plot the field distributions in the entire structure in Fig. 5. It is apparent that a good coupling between the PPCHWG and SWG is realized.

Additionally, the investigation of the coupling effects in our proposed 2D structures allows to provide a lot of useful information for guiding the design of couplers with less computing time, and supply the references in the applications to the corresponding 3D case. We have carried out the related calculations in terms of the 3D FDTD method. The distributions of 3D version of the steady electric field intensity over a xz cross-section-plane (noted that the transmission is measured at (x, y, z)=(0, 9, 0) μm in the central part of the xz cross-section-plane) when the coupling is made from the SWG to the PPCHWG is presented in Fig. 6. The wavelength of the incident field corresponds to $\lambda = 1.65$ μm and the units on the axis are grid cells (dx, dy, dz): $dx = dy = dz = 20$ nm, slab height $h = 10a$, $a = 540$ nm. It is clearly seen that the electric field is well confined in the output end of SWG, and the transmission reaches 83%. The out-of-plane radiation losses are evaluated to be 10% more than the 2D case (the transmission is 93%), as plotted in Fig. 5. The reason is that because the 3D defect mode has a smaller bandwidth compared with the 2D case [21], thus, in the 3D case, the group velocity is lowered and so is the k-vector phase mismatch with the reflected wave. On the basis of simulations, it is found that if the size of the sample along the vertical direction, i.e., the z-axis, is sufficiently large, for instance, the height h is greater than $10a$, the detrimental influence of the out-of-plane radiation can become less.

Basically, the detailed analysis and comparisons of the properties between the 3D structures (i.e., a structure with finite vertical height consisting of the periodic repeated stack of the 2D PC) generated by other known approaches of PPCWGs [22–25] with our proposed structure of PPCHWG are quite complex problems. We prefer to further study them in the future works.

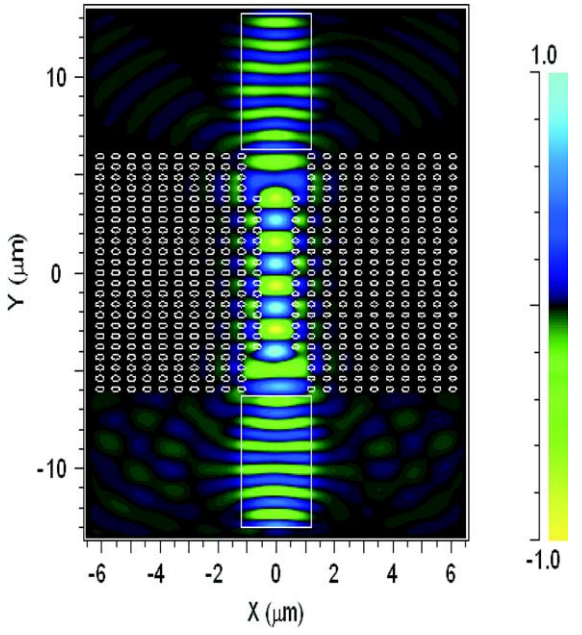

Fig. 5. Field distributions in the entire structure with a width of PPCHWG of $w = dx = 1.44a$.

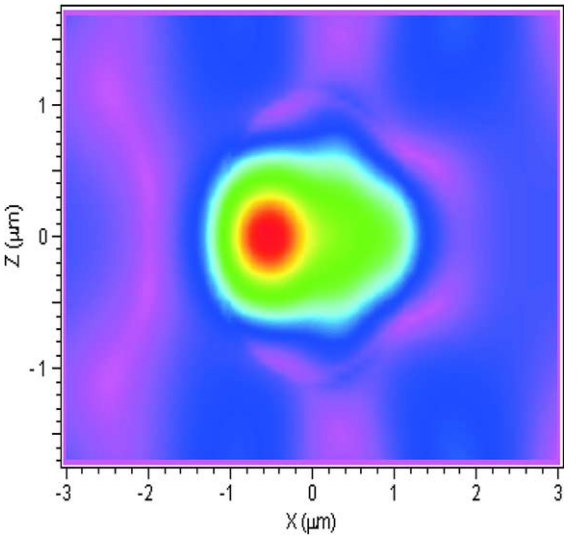

Fig. 6. Distributions of 3D version of the steady electric field intensity over a xz cross-section-plane, which is measured at $(x, y, z) = (0, 9, 0)$ in the central part of the xz cross-section-plane, when the coupling is from the SWG to the PPCHWG. The wavelength of incident field corresponds to $\lambda = 1.65$ μm and the units on the axis are grid cells (dx, dy, dz): $dx = dy = dz = 20$ nm, the slab height $h = 10a$, $a = 540$ nm.

In conclusion, we propose a planar PC heterostructure waveguide composed of two semi-infinite PCs with different structural parameters, contacted together. This PPCHWG is connected to two external SWGs. PPCHWGs possess the merits of the flexible control of the creation of localized defect states within the PC band gap and the wave guide width can be continuously changed. We investigate the coupling efficiency in the system and find that it can be significantly enhanced by improving the mode matching from a SWG to a PPCHWG via the optimal design of the coupling region structure. By calculating the transmittance at the output end of SWG, we find that the proposed structure can have high coupling efficiency and relax the fabrication tolerance. The maximum transmittance exceeds 90% for a wavelength near 1.65 μm. It is worth noting that the PPCHWGs arrive at high transmission efficiency without introducing any line defects for achieving the mode matching at the entrance and exit terminals of PPCHWGs. Besides, the width of PPCHWGs can be flexibly controlled by changing the separation of two component PCs in PC heterostructures.

Acknowledgement

This work was supported by the National Science Council of Republic of China to offer us financial support through the Grant No. NSC94-2112-M-234-001.

References

[1] H. Kosaka, T. Kawashima, A. Tomita, M. Notomi, T. Tamamura, T. Sato, S. Kawakami, Appl. Phys. Lett. 74 (1999) 1370.
[2] H. Kosaka, T. Kawashima, A. Tomita, M. Notomi, T. Tamamura, T. Sato, S. Kawakami, Appl. Phys. Lett. 74 (1999) 1212.
[3] A.R. McGurn, Phys. Rev. B 61 (2000) 13235.
[4] H. Kosaka, T. Kawashima, A. Tomita, M. Notomi, T. Tamamura, T. Sato, S. Kawakami, Phys. Rev. B 58 (1998) 10096.
[5] M. Tokushima, H. Kosaka, A. Tomita, H. Yamada, Appl. Phys. Lett. 76 (2000) 952.
[6] A. Talneau, Ph. Lalanne, M. Agio, C.M. Soukoulis, Opt. Lett. 27 (2002) 1522.
[7] P. Sanchis, A. Talneau, Opt. Express 10 (2002) 354.
[8] P. Sanchis, J. Marti, J. Blasco, A. Martinez, A. Garcia, Opt. Express 10 (2002) 1391.
[9] Jianhua Jiang, Jingbo Cai, Gregory P. Nordin, Lixia Li, Opt. Lett. 28 (2003) 2381.
[10] L.L. Lin, Z.Y. Li, Phys. Rev. B 63 (1998) 03310.
[11] J. Agi, E.R. Brown, O.B. Mcmahon, C. Dill, K.J. Malloy, Electron. Lett. 30 (1994) 2166.
[12] C. Zhang, F. Qiao, J. Wan, J. Zi, J. Appl. Phys. 87 (2000) 3174.
[13] Yuan-Fong Chau, Tzong-Jer Yang, Ben-Yuan Gu, Jpn. J. Appl. Phys. 43 (2004) L1064.
[14] Yuan-Fong Chau, Tzong-Jer Yang, Win-Der Li, Appl. Opt. 43 (2004) 6656.
[15] See <http://ab-initio.mit.edu/mpb>.
[16] Yuan-Song Zhou, Ben-Yuan Gu, Fu-He Wang, J. Phys. Condens. Matter 15 (2003) 4109.
[17] Yuan-Song Zhou, Ben-Yuan Gu, Fu-He Wang, Eur. Phys. J. B 37 (2004) 293.
[18] A. Taflove, Computational Electrodynamics, Artech, Norwood, MA, 2000.
[19] J.P. Berenger, J. Comput. Phys. 114 (1994) 185.
[20] P. Sanchis, J. Marti, A. Garcia, A. Martineand, J. Blasco, Electron. Lett. 38 (2002) 961.
[21] P. Bienstman, S. Assefa, S.G. Johnson, J.D. Joannopoulos, G.S. Petrich, L.A. Kolodziejski, J. Opt. Soc., Am. B 20 (2003) 1817.
[22] W.T. Lau, S. Fan, APL 81 (2002) 3915.
[23] M. Loncar, J. Vuckovic, A. Sherer, J. Opt. Soc., Am. B 18 (2001) 1362.
[24] S.G. Johnson, P.R. Villeneuve, Shanhui Fan, J.D. Joannopoulos, Phys. Rev. B 62 (2000) 8212.
[25] T. Sondergaard, A. Lavrinenko, Opt. Commun. 203 (2002) 263.